NASA TM-81968

NASA Technical Memorandum 81968

NASA-TM-81968 19810015327

LATERAL ATTENUATION OF HIGH-BY-PASS RATIO ENGINED AIRCRAFT NOISE

WILLIAM L. WILLSHIRE, JR.

APRIL 1981

NASA
National Aeronautics and
Space Administration

Langley Research Center
Hampton, Virginia 23665

SUMMARY

A flight experiment was conducted to investigate the lateral attenuation of high-by-pass ratio engined airplanes. A B-747 was flown at low altitudes over the ends of two microphone arrays. One array covering a lateral distance of 1600 m consisted of 14 microphones positioned over grass. The second array covered a lateral distance of 1200 m and consisted of 6 microphones positioned over a concrete runway. Sixteen runs were flown at altitudes ranging from 30 to 960 m.

The acoustic information recorded in the field has been reduced to one-third-octave band spectral time histories and synchronized with tracking and weather information. Lateral attenuation as a function of elevation angle has been calculated in overall, A-weighted, tone-corrected perceived noise level, and effective perceived noise level units.

The B-747 results are compared with similar results for a turbojet-powered T-38 airplane and the SAE-recommended lateral attenuation prediction procedure. Less lateral attenuation was measured for the B-747 than for the T-38. The B-747 lateral attenuation values also fell below the SAE curve. The B-747 source spectra have considerable energy in the low and high frequencies. The low frequency content was not strongly affected by ground effects or atmospheric absorption and became dominant in the measured spectra. The amount of lateral attenuation (in terms of integrated metrics) of a particular noise source appears to depend strongly on the spectral content of the noise source and the frequency dependence of the ground effects.

INTRODUCTION

Lateral attenuation of aircraft noise is a significant factor in calculating the community noise exposure around airports. The FAA, other international air transportation authorities, and community planners require sound technical methods upon which to base noise contour calculations. Therefore, the SAE A-21 Aircraft Noise Committee in the past year collected all the existing available data on lateral attenuation of aircraft to develop an interim method of lateral attenuation prediction which has been published as an Aerospace Information Report (ref. 1). One of the key sets of data was the T-38 experiment (refs. 2 and 3) which contains over 400 lateral attenuation measurements. At the same time, the committee recognized that in the available lateral attenuation data base, very few data points were associated with high-by-pass-ratio engines. The B-747 lateral attenuation experiment was undertaken to fill this gap in the available lateral attenuation data base.

The purpose of this report is to present the lateral attenuation results of the B-747 experiment in terms of integrated metrics. The experiment, including data reduction, is discussed in the next section of this report, followed by sections on the data analysis and results. The final sections of the paper include discussions of the results and concluding remarks.

EXPERIMENT

Test Site and Aircraft

The flight experiment was conducted on November 2, 1980, at NASA Wallops Flight Center, Wallops Island, Virginia. The test aircraft was an American Airlines Boeing 747-123 (tail number N9666) with JT9D-3A engines. The engines had fixed inlet lips and no splitters. The test airplane was flown at altitudes of 30, 60, 120, 240, 480, and 960 m over the ends of two microphone arrays. One array covering a lateral distance of 1600 m consisted of 14 microphones positioned over grass. The second array covered a lateral distance of 1200 m and consisted of 6 microphones positioned over a concrete runway. The majority of the microphones were supported 1.2 m above the ground plane.

A photograph of the experimental site is given as figure 1. The flight path was above runway 10-28 from the west toward the east. The microphone arrays were positioned along runway 04-22 and the grassy area between runway 04-22 and its taxiway. A detailed description of the runways and the grassy areas is given in reference 3. A diagram of the microphone layout is presented as figure 2 which includes the microphone numbers and heights. The coordinates of the microphones are given in Table I in the data reduction coordinate system (defined in the data reduction section).

Figure 3 is a photograph of the American Airlines B-747 on the ground at Wallops and figure 4 is a photograph of the airplane flying at 30 m over the microphone arrays. The airplane was tracked with a laser tracker. The laser reflector housing equipped with a backup C-band radar transponder and battery pack was mounted underneath the port wing tip near the trailing edge of the wing. Figure 5 consists of close-up photographs of the assembled laser reflector housing with the transponder and the battery pack. The installation of the laser housing which weighed 29.9 lbs (with the transponder and battery pack) is shown in figure 6.

Sixteen runs were completed; the run conditions are listed in Table II. The airplane was flown with all four engines at a constant engine pressure ratio with the landing gear, gear doors, and flaps deployed. The engine and airplane conditions as recorded in the cockpit are given in Table III.

Weather information was gathered from four weather stations positioned along the microphone arrays. One of the four stations was mounted on a mechanical traversing arm to accurately measure weather parameter profiles up to a height of 2 m. A retrievable balloon was used to raise a fifth weather station to make higher weather parameter profiles with less spatial resolution.

Acoustic Data Reduction

The acoustic data collected for the 16 runs have been reduced to one-third-octave band spectral time histories and synchronized with the tracking and weather information. The acoustic data were reduced with an averaging time of 1/4 second. The frequency range of the one-third-octave band analysis was from 20 Hz to 10 kHz. The recorders were turned on in the field for each run when the airplane was incoming and just beyond two miles from the intersection of runways 04-22 and 10-28. Turning the recorders on early provided ambient measurement for each microphone for each run. Each microphone system (see figure 7) was tested before going into the field to insure that the equipment operated within the manufacturer's specifications. A pre- and a post-calibration was performed on each system in the field. The pre-calibration involved an amplitude and a pink noise calibration. The post-calibration was a check on the stability of the amplitude calibration. In the data reduction process, the pink noise calibration was used to insure a flat frequency response of the record/playback systems. The acoustic data were not corrected to standard day weather conditions.

Tracking Data Reduction

The laser tracker lost track of the airplane for a brief period due to the close proximity of the flight path to the tracker, coupled with the slew rate of the tracker pedestal. The possibility of this occurring was known (refs. 2 and 3), but design requirements of the experiment excluded other possible microphone/flight path layouts. The average gap per run was 11 seconds. During the tracking data reduction, straight lines were computed to fill the gaps and a 21-point sliding average was performed on each flight track.

Tracking information was recorded every 1/10 second. The tracking data were transformed from spherical coordinates referenced to the laser tracker to Cartesian coordinates referenced to the intersection of runways 04-22 and 10-28. The Cartesian coordinate system, referred to as the data reduction coordinate system, is illustrated in figure 8. The tracking point on the airplane was changed during the data reduction from the laser housing mounted on the port wing tip to the geometric center of the four engine exhausts.

Weather Data Reduction

The weather data from the five weather stations have been organized and transformed where needed into a consistent set of data in metric units. Weather data from the balloon weather station are illustrated in figure 9. Profiles of temperature, relative humidity, and wind speed are given in the figure. The data were taken at approximately the time of run 8. The wind was generally from the northwest during the test.

DATA ANALYSIS

The method used to calculate lateral attenuation is a comparative method in which a one-third-octave band spectrum from a particular microphone, called the measurement microphone, is compared for the same run with a one-third-octave band spectrum from a second microphone, referred to as the reference microphone, positioned underneath the flight path. The reference spectrum is brought to the same slant range in terms of spherical spreading and atmospheric absorption as the measurement spectrum. The two spectra to be compared are selected from their respective microphone time histories using a source directivity angle criterion. The angle criterion insures that both spectra are emitted with the same source emission angle and propagated over the same surface. Lateral attenuation is defined as the difference between the reference spectrum and the measurement spectrum.

Single Spectra Analysis

For overall, A-weighted, and tone corrected perceived noise level analysis, the one-third-octave band spectra emitted with an emission directivity angle of 122.5 deg, (referenced to the forward inlet direction, see fig. 10) are selected to be the reference and measurement spectra. Because of the oblique angle between the microphone arrays and the flight track in the experiment, the sound emitted from the airplane at an emission angle of 122.5 deg propagated parallel to the microphone arrays. The portions of the microphone signals selected with the 122.5 deg angle criterion have the same source origin and propagated over the same surface. For a particular measurement microphone and run, a receive time is calculated for the microphone for the sound emitted at 122.5 deg. The two one-third-octave band spectra located on either side of this time in the microphone time history are averaged. The average spectrum has an effective averaging time of one-half second and is integrated to form the desired metric. For the same run, a reference microphone, usually microphone 1, is chosen and an average one-third-octave band spectrum is obtained in the same manner. Before integrating to form the same metric, spherical spreading and atmospheric absorption corrections are applied to bring the reference spectrum to the same slant range as the measurement spectrum. Atmospheric absorption corrections are calculated using the American National Standards Institute (ANSI) standard method for the determination of molecular absorption (ref. 4). The measurement value is subtracted from the reference value to form the lateral attenuation result. A positive lateral attenuation value denotes an attenuation.

Spectral Time History Analysis

For effective perceived noise level, EPNL, analysis, the measurement value is calculated directly from the measurement microphone time history. The corresponding reference EPNL value for the same run is calculated in the following manner: The emission angles for each one-third-octave band spectra of the measurement microphone time history are calculated. Each one-third-octave band spectrum in the measurement time history is replaced with a spectrum from the reference microphone for the same emission angle. The reference microphone spectra are corrected to the same slant range as the measurement spectra they replace. In this manner a reference time history congruous to the measurement time history is formed and is used in the reference EPNL calculation. The measurement EPNL value is subtracted from the reference EPNL value to yield a lateral attenuation measurement.

In order to make the reference EPNL calculation more efficient, average reference spectra are used. Instead of replacing the spectra of a particular measurement time history with spectra from the reference microphone for the same run, the measurement spectra are replaced with the average reference spectra. The average reference spectra are formed by averaging spectra for microphone 1 for the first ten runs. To represent the source emission angles from 0 to 180 degrees, 22 average spectra are used. The average reference spectrum of the 22 closest to the emission angle of a particular measurement spectrum is used to replace that measurement spectrum to form the reference time history.

Results

Overall sound pressure level, SPL, A-weighted sound pressure level, LA, tone corrected perceived noise level, PNLT, and EPNL average results as a function of elevation angle are given in figures 11-14 respectively. Data are given for all the 1.2 m microphones positioned over grass (microphones 1, 3, 4, 6, 7, 8, 10, 11, and 13) for runs 1-12. The data for individual microphones for similar runs are averaged. For example, the results for microphone 4 for runs 1, 2, 7, and 8, all 30 m runs, are averaged to form a single data point. The results for runs 3, 4, 9, and 10 (60 m runs), for runs 5 and 6 (120 m runs), and for runs 11 and 12 (240 m runs) are also averaged. The reference microphone for all the results was microphone 1, the closest 1.2 m microphone positioned over grass to the airplane flight track. The data plotted in figures 11-14 are listed in Table IV along with the average results for the 10 m microphones positioned over grass, microphones 5, 9, and 12. Also included in Table IV are the individual reference and measurement integrated metric values. Measurement EPNL values for microphone 20 for all the runs are listed in Table V. The elevation angles and slant ranges used in the figures and the tables are the closest approach values.

In figures 15 - 18 the results of least-squares fits of the data presented in figures 11 - 14 are given and compared with similar T-38 excess ground attenuation experimental results. The least-squares fits of the B-747 and the T-38 results are second order and constrained to be 0 at 90 deg. The least-squares fit coefficients for the B-747 results are given in Table VI. No overall T-38 results have been calculated, therefore none are given in figure 15. The long range (SAE AIR 1751) lateral attenuation prediction curve is included in figure 18 for comparison with the B-747 and the T-38 EPNL results.

DISCUSSION OF RESULTS

The measured lateral attenuation was less for the B-747 experiment than for the T-38 experiment. The B-747 EPNL results also fell beneath the AIR 1751 long range lateral attenuation prediction curve. The comparison of the long range curve and the B-747 EPNL results is valid for small elevation angles because the slant ranges associated with the small angle data are greater than the 926 m criterion given in the AIR. A reason that less lateral attenuation was measured in the B-747 experiment is the acoustic energy distribution in the B-747 source spectra.

The B-747 source spectra have considerable energy content in the low and high frequencies. An average estimate free-field source spectrum for the B-747 is illustrated in figure 19 for an emission directivity angle of 122.5 degrees. The spectrum in figure 19 is an average of 50 spectra; spectra were obtained for an emission angle of 122.5 deg for microphones 1, 2, 15, 16, and 17 for runs 1-10. A ground effects prediction (ref. 2) was made for each spectrum and used to remove the influence of ground effects before averaging. A strong fan tone at 4 kHz is observed in the spectrum as well as considerable acoustic energy in the one-third-octave bands less than 100 Hz.

The fan tone is rapidly attenuated by atmospheric absorption because of its high frequency. The effects of ground attenuation are the greatest in the frequency range of 200 to 400 Hz (ref. 2). The acoustic energy below 100 Hz is not affected strongly by ground attenuation or atmospheric absorption and remains dominant in the measurement spectra. An average measurement spectrum for microphone 10 for the 30 m runs and an emission angle of 122.5 deg is shown in figure 20. The fan tone has been greatly reduced, the ground dip is observed above 100 Hz, and the energy below 100 Hz dominates the spectrum. Because of the low frequency penalty of A-weighting, lateral attenuation of a source spectrum with low frequency content in A-weighted units would be expected to be greater than lateral attenuation measured in overall units. This is clearly observed in the B-747 results (figs. 15 and 16).

The amount of lateral attenuation a particular noise source will experience is dependent on the spectral content of the noise source. A larger amount of integrated lateral attenuation was measured in the T-38 experiment than in the B-747 experiment because the spectral shape of the T-38 noise source more closely matched the spectral shape of the ground effects. In figure 21 an estimate of the T-38 free-field source spectrum is compared with the B-747 source spectrum given in figure 19. The T-38 spectrum was obtained in the same way the B-747 spectrum was obtained. Where the T-38 noise source had a lot of acoustic energy, the ground effects were the largest. The influence of the ground effects was, therefore, greater on the T-38 data in the integrated analysis. The match between the ground effects and the spectral shape of the B-747 data was not as good and the resulting integrated lateral attenuation values were smaller.

The majority of the data that went into the lateral attenuation prediction curve of AIR 1751 were not for high-by-pass engined airplanes. The higher frequency noise content of the smaller engined airplanes resulted in a better match with the ground attenuation frequency dependence and, therefore, in more measured lateral attenuation in the integrated metrics. One set of data for a B-747 was presented at the Lateral Attenuation Plotting Session and incorporated in the AIR. The previous B-747 data fall below the AIR prediction curve and are in line with the Wallops B-747 data (see fig. 22).

CONCLUDING REMARKS

Lateral attenuation in integrated metrics for a high-by-pass ratio engined airplane, a B-747, were measured in flight and found to be less than for a turbojet-powered airplane, a T-38. The high-by-pass ratio results also fell beneath the SAE recommended interim lateral attenuation prediction curve. The lateral attenuation results of the present study were in agreement with a previous set of limited data for a B-747.

The measured lateral attenuation differed for the two airplanes because of spectral differences in their noise spectra. The maximum acoustic energy of the T-38 source spectrum was located in the same frequency range, 100 - 500 Hz, as the largest ground effects. In the case of the T-38, larger values of lateral attenuation were measured because ground effects greatly reduced the dominant frequency bands of the T-38 source spectrum. The B-747 source spectrum had considerable energy content less than 100 Hz. This low frequency acoustic energy was not affected greatly by ground effects or absorption. The low frequency content of the B-747 noise source remained in the measurement spectra. The integrated values of the measurement spectra were dominated by the low frequency content and less lateral attenuation was measured. The amount of lateral attenuation in integrated metrics of a particular noise source depends strongly on the spectral content of the noise source and the frequency dependence of the ground effects.

Langley Research Center
National Aeronautics and Space Administration
Hampton, VA 23665
April 15, 1981

REFERENCES

1. Anon.: Prediction Method for Lateral Attenuation of Airplane Noise During Takeoff and Landing. Aerospace Information Report 1751, SAE, March 1981.

2. Willshire, W. L., Jr.: Assessment of Ground Effects on the Propagation of Aircraft Noise: The T-38A Flight Experiment. NASA TP 1747, 1980.

3. Willshire, William L., Jr.; and Hilton, David A.: Ground Effects on Aircraft Noise. NASA TM 80185, 1979.

4. Method for the Calculation of the Absorption of Sound by the Atmosphere. ANSI S1.26-1978 (ASA 23-1978). American National Standards Institute, Inc., June 23, 1978.

mic no.	x, m	y, m	z, m
1	−77.23	53.34	1.20
2	−100.00	56.39	10.00
3	−246.70	53.34	1.20
4	−462.99	53.34	1.20
5	−462.99	56.39	10.00
6	−755.45	71.17	1.20
7	−926.01	79.25	1.20
8	−1149.61	79.25	1.20
9	−1149.61	82.30	10.00
10	−1388.97	79.25	1.20
11	−1606.81	79.25	1.20
12	−1606.81	82.30	10.00
13	−1851.96	79.25	1.20
14	0.0	0.0	1.20
15	−100.00	−3.05	0.0
16	−100.00	0.0	1.20
17	−100.00	3.05	10.00
18	−926.01	0.0	1.20
19	−1388.97	0.0	1.20
20	250.00	53.34	1.20

TABLE 1. Microphone Coordinates

RUN	ALTITUDE, m
1	30
2	30
3	60
4	60
5	120
6	120
7	30
8	30
9	60
10	60
11	240
12	240
13	480
14	480
15	960
16	960

TABLE 2. Test Matrix.

TM1.TVG

RUN	EPR				N_1				ALT, ft		VTAS kts	TEMP deg C	
	1	2	3	4	1	2	3	4	RAD	BAR		STA	TOT
1	1.20	1.20	1.20	1.20	.79	.80	.80	.76	120	120	173	10	14.2
2	1.23	1.20	1.20	1.18	.80	.80	.80	.75	120	120	179	10	14.4
3	1.20	1.20	1.20	1.21	.79	.77	.79	.77	240	240	167	10	13.5
4	1.21	1.21	1.21	1.21	.79	.78	.80	.78	230	240	169	10	13.6
5	1.21	1.21	1.22	1.20	.78	.78	.80	.76	450	420	168	9	13.2
6	1.21	1.20	1.21	1.20	.79	.77	.79	.77	430	420	163	9	12.8
7	1.21	1.20	1.20	1.21	.79	.77	.79	.77	130	160	174	10	13.7
8	1.20	1.20	1.20	1.20	.78	.77	.79	.76	120	160	171	10	13.7
9	1.20	1.20	1.19	1.21	.79	.77	.78	.77	200	260	181	10	13.8
10	1.20	1.20	1.20	1.20	.78	.77	.79	.76	210	240	167	10	12.9
11	1.20	1.20	1.21	1.19	.78	.76	.78	.76	750	800	161	8	12.0
12	1.20	1.20	1.20	1.20	.78	.76	.78	.76	780	820	163	8	12.2
13	1.20	1.20	1.20	1.20	.77	.75	.77	.75		1600	157	6	9.9
14	1.20	1.20	1.20	1.20	.77	.76	.78	.76		1620	157	6	9.6
15	1.20	1.20	1.20	1.20	.78	.76	.79	.76		3200	176	2	6.0
16	1.21	1.21	1.21	1.20	.78	.76	.78	.75		3200	159	2	5.7

NOTE: For all runs the gear was down with doors open and flaps set at 30 deg. For run 9 the flaps were blown back to a 25 deg setting.

TABLE 3. Engine Run Conditions

Average 747 Lateral Attenuation Results for runs 1, 2, 7, and 8

MEA MIC	MEA SPL dB	REF SPL dB	MEA LA dB	REF LA dB	MEA PNLT dB	REF PNLT dB	MEA EPNL dB	REF EPNL dB	SLANT RANGE m	LOOK ANGLE deg	LATERAL ATTENUATION SPL dB	LATERAL ATTENUATION LA dB	LATERAL ATTENUATION PNLT dB	LATERAL ATTENUATION EPNL dB
1	125.7	125.7	101.0	101.0	119.1	119.1	114.0	113.4	55.4	35.2	0.0	0.0	0.0	-0.7
2	104.7	104.2	99.6	99.2	115.1	117.3	114.3	113.0	65.0	22.1	-0.6	-0.5	-0.8	-1.3
3	94.8	94.1	87.4	86.2	105.8	103.1	103.6	104.6	188.0	9.8	-0.7	-1.2	-0.6	1.0
4	86.1	87.8	76.5	77.7	92.4	92.1	93.7	98.6	369.6	4.9	1.8	1.2	-0.3	4.9
5	85.6	87.9	79.1	77.7	95.6	92.2	95.5	98.5	367.2	3.8	2.3	-1.3	-3.4	3.0
6	81.9	83.3	70.3	71.7	85.1	85.5	88.0	93.7	607.6	3.0	1.4	1.4	0.4	5.6
7	79.8	81.4	67.7	69.3	83.0	83.0	84.5	91.6	747.8	2.4	1.6	1.6	0.0	7.1
8	76.7	79.3	61.5	66.6	75.3	80.2	81.6	89.6	937.3	1.9	2.7	4.9	4.9	8.0
9	76.0	79.4	63.7	66.6	77.8	80.2	82.5	89.6	935.4	1.5	3.3	2.9	2.4	7.1
10	75.3	77.5	60.5	64.3	73.9	77.5	80.3	87.8	1140.1	1.6	2.2	3.7	3.6	7.4
11	73.4	76.2	57.0	62.5	72.0	74.5	77.9	86.0	1324.8	1.4	2.7	5.5	4.4	8.1
12	74.1	76.2	61.0	62.5	73.5	74.5	81.1	86.2	1323.0	1.1	2.1	1.5	1.0	5.1
13	73.5	74.8	57.0	60.7	69.8	72.3	78.0	84.5	1532.6	1.2	1.3	3.7	2.4	6.4

Average 747 Lateral Attenuation Results for runs 3, 4, 9, and 10

MEA MIC	MEA SPL dB	REF SPL dB	MEA LA dB	REF LA dB	MEA PNLT dB	REF PNLT dB	MEA EPNL dB	REF EPNL dB	SLANT RANGE m	LOOK ANGLE deg	LATERAL ATTENUATION SPL dB	LATERAL ATTENUATION LA dB	LATERAL ATTENUATION PNLT dB	LATERAL ATTENUATION EPNL dB
1	104.2	104.2	101.9	101.9	120.5	120.5	112.5	111.2	77.2	47.4	0.0	0.0	0.0	-1.3
2	104.4	103.8	100.5	101.4	118.9	119.9	112.4	111.6	80.6	37.8	-0.6	0.9	1.0	-0.8
3	95.2	94.7	88.2	89.9	106.7	107.6	104.7	104.3	192.8	17.1	-0.5	1.6	0.9	-0.4
4	87.5	88.3	78.3	81.0	94.8	96.3	94.2	98.0	369.3	8.8	0.9	2.7	1.5	3.8
5	86.1	88.4	78.7	81.1	95.4	96.4	95.7	98.0	366.2	7.7	2.3	2.4	1.1	2.2
6	83.2	83.7	72.2	74.7	87.3	88.7	83.8	93.1	604.0	5.4	0.5	2.5	1.4	4.2
7	80.7	81.8	69.7	72.1	83.9	85.9	85.3	90.9	742.8	4.4	1.0	2.5	2.1	5.6
8	77.7	79.7	65.9	69.3	78.6	83.1	82.5	88.9	930.7	3.5	1.9	3.4	4.5	6.4
9	77.0	79.7	66.0	69.4	80.3	83.1	83.1	88.9	928.5	3.0	2.7	3.3	2.8	5.8
10	75.3	77.8	61.1	66.9	74.4	80.7	79.9	87.2	1132.1	2.9	2.5	5.8	6.3	7.4
11	73.4	76.4	59.0	65.0	71.9	77.4	78.2	85.5	1315.5	2.5	3.0	6.1	5.4	7.3
12	72.7	76.4	61.3	65.0	73.9	77.4	80.1	85.7	1313.4	2.2	3.8	3.8	3.4	5.6
13	72.6	75.0	58.0	63.2	70.4	75.0	77.2	84.0	1521.9	2.1	2.4	5.2	4.6	6.9

TABLE 4. Average Lateral Attenuation results for 30, 60, 120, and 240 m Runs.

Average 747 Lateral Attenuation Results for runs 5 and 6

MEA MIC	MEA SPL dB	REF SPL dB	MEA LA dB	REF LA dB	MEA PNLT dB	REF PNLT dB	MEA EPNL dB	REF EPNL dB	SLANT RANGE m	LOOK ANGLE deg	LATERAL ATTENUATION SPL dB	LA dB	PNLT dB	EPNL dB
1	98.7	98.7	95.7	95.7	113.8	113.8	108.4	107.1	133.0	54.0	0.0	0.0	0.0	-1.3
2	100.0	98.9	96.8	95.9	115.6	114.0	109.0	107.5	131.0	49.9	-1.1	-0.9	-1.6	-1.5
3	95.1	93.5	88.7	88.8	106.7	105.9	104.0	103.1	219.7	29.3	-1.7	0.1	-0.7	-0.9
4	88.5	88.1	79.2	81.4	95.7	97.0	95.5	97.8	380.2	16.4	-0.5	2.1	1.3	2.4
5	87.6	88.2	79.3	81.5	96.6	97.2	96.8	97.8	375.7	15.5	0.6	2.2	0.6	1.0
6	84.8	83.6	72.1	75.4	86.4	89.4	89.7	93.1	604.2	10.3	-1.2	3.2	3.0	3.3
7	81.0	81.7	70.1	72.8	83.8	86.4	87.0	91.0	738.6	8.4	0.8	2.6	2.6	4.0
8	77.8	79.6	64.8	70.0	77.5	83.4	83.5	89.0	921.6	6.7	1.8	5.2	5.9	5.5
9	75.5	79.7	65.3	70.0	78.7	83.5	83.8	89.0	918.8	6.3	4.2	4.7	4.7	5.2
10	75.8	77.8	64.3	67.5	77.4	81.0	80.3	87.3	1118.3	5.5	1.9	2.7	3.7	7.1
11	74.6	76.4	62.8	65.6	75.2	77.1	77.7	85.6	1297.8	4.8	1.8	2.8	2.0	7.9
12	74.1	76.4	63.8	65.6	76.7	77.2	82.1	85.8	1295.3	4.4	2.3	1.8	0.5	3.7
13	73.4	75.0	60.6	63.8	72.5	75.2	77.4	84.2	1500.1	4.1	1.6	3.2	2.8	6.7

Average 747 Lateral Attenuation Results for runs 11 and 12

MEA MIC	MEA SPL dB	REF SPL dB	MEA LA dB	REF LA dB	MEA PNLT dB	REF PNLT dB	MEA EPNL dB	REF EPNL dB	SLANT RANGE m	LOOK ANGLE deg	LATERAL ATTENUATION SPL dB	LA dB	PNLT dB	EPNL dB
1	93.1	93.1	87.5	87.5	104.1	104.1	102.5	102.9	235.9	57.9	0.0	0.0	0.0	0.4
2	93.9	93.4	88.8	88.0	105.9	104.8	103.7	102.9	227.4	57.8	-0.4	-0.8	-1.1	-0.8
3	92.2	91.6	86.5	85.5	104.0	101.6	101.6	100.7	273.6	46.9	-0.6	-1.1	-2.4	-0.9
4	89.0	89.0	80.3	80.6	96.6	95.2	96.2	96.9	399.5	30.0	-1.0	0.3	-1.4	0.6
5	88.2	88.1	79.9	82.8	96.0	95.4	97.0	96.8	393.1	29.3	-0.1	0.9	-0.5	-0.2
6	84.1	84.0	73.1	75.2	87.6	88.8	91.4	92.6	609.0	19.1	-0.1	2.1	1.2	1.3
7	81.8	82.2	70.1	72.8	83.0	86.2	88.8	90.7	740.7	15.6	0.3	2.7	3.2	1.9
8	79.9	80.1	67.8	70.0	80.9	83.4	85.6	88.8	922.7	12.5	0.2	2.2	2.5	3.2
9	78.6	80.1	66.8	70.1	79.7	83.5	85.4	88.9	919.0	12.1	1.5	3.2	3.8	3.4
10	76.5	78.2	63.9	67.6	76.7	81.1	82.7	87.2	1120.4	10.3	1.7	3.7	4.3	4.5
11	74.1	76.8	60.5	65.7	72.4	77.5	78.9	85.4	1301.9	8.8	2.7	5.2	5.2	6.5
12	73.4	76.8	62.9	65.8	75.5	77.6	81.9	85.6	1298.8	8.5	3.5	2.9	2.1	3.7
13	73.4	75.4	56.7	63.9	70.3	75.6	77.9	83.9	1507.1	7.6	2.0	7.2	5.4	6.1

TABLE 4. – continued.

RUN NO.	SLANT RANGE m	ELEVATION ANGLE deg	EPNL dB
1	137.6	12.6	109.6
2	137.6	12.6	105.3
3	147.1	24.1	106.0
4	147.1	24.1	105.4
5	180.1	41.8	105.7
6	180.1	41.8	106.1
7	137.6	12.6	105.1
8	137.6	12.6	105.6
9	147.1	24.1	104.9
10	147.1	24.1	105.2
11	275.0	60.8	105.9
12	275.0	60.8	106.0
13	498.4	74.4	101.7
14	498.4	74.4	98.2
15	969.4	82.0	97.0
16	969.4	82.0	93.6

TABLE 5. Measurement EPNL Values for Mic 20.

	C0	C1	C2
SPL	3.063	−2.887	0.491
LA	4.523	−0.899	−1.023
PNLT	3.840	−0.475	−1.176
EPNL	8.818	−4.536	−0.611

where: $Y = C0 + C1*X + C2*X^2$

with X = LOG(Elevation Angle, deg)

TABLE 6. B−747 Least-squares Fit Coefficients

TM2.TVG

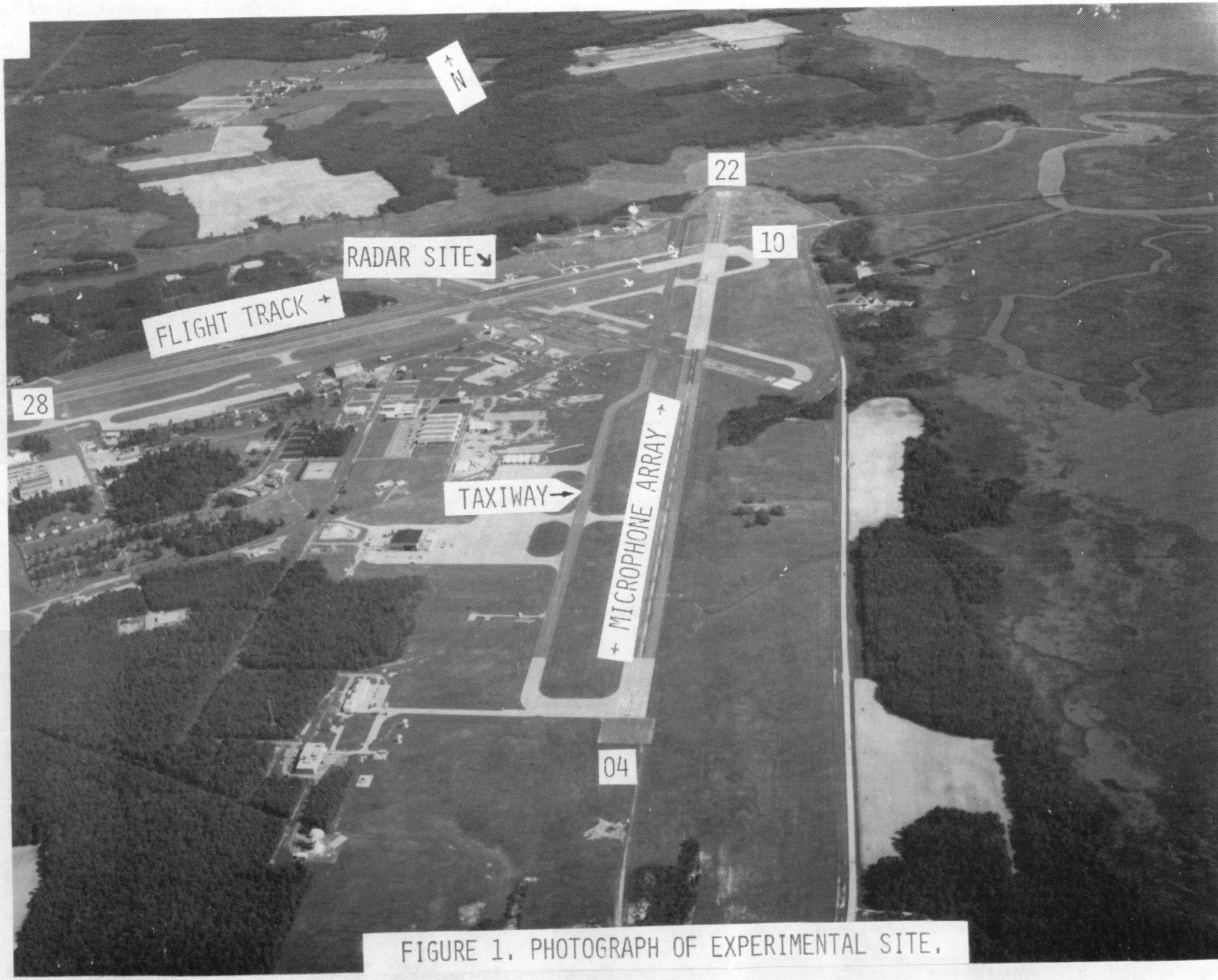

FIGURE 1. PHOTOGRAPH OF EXPERIMENTAL SITE.

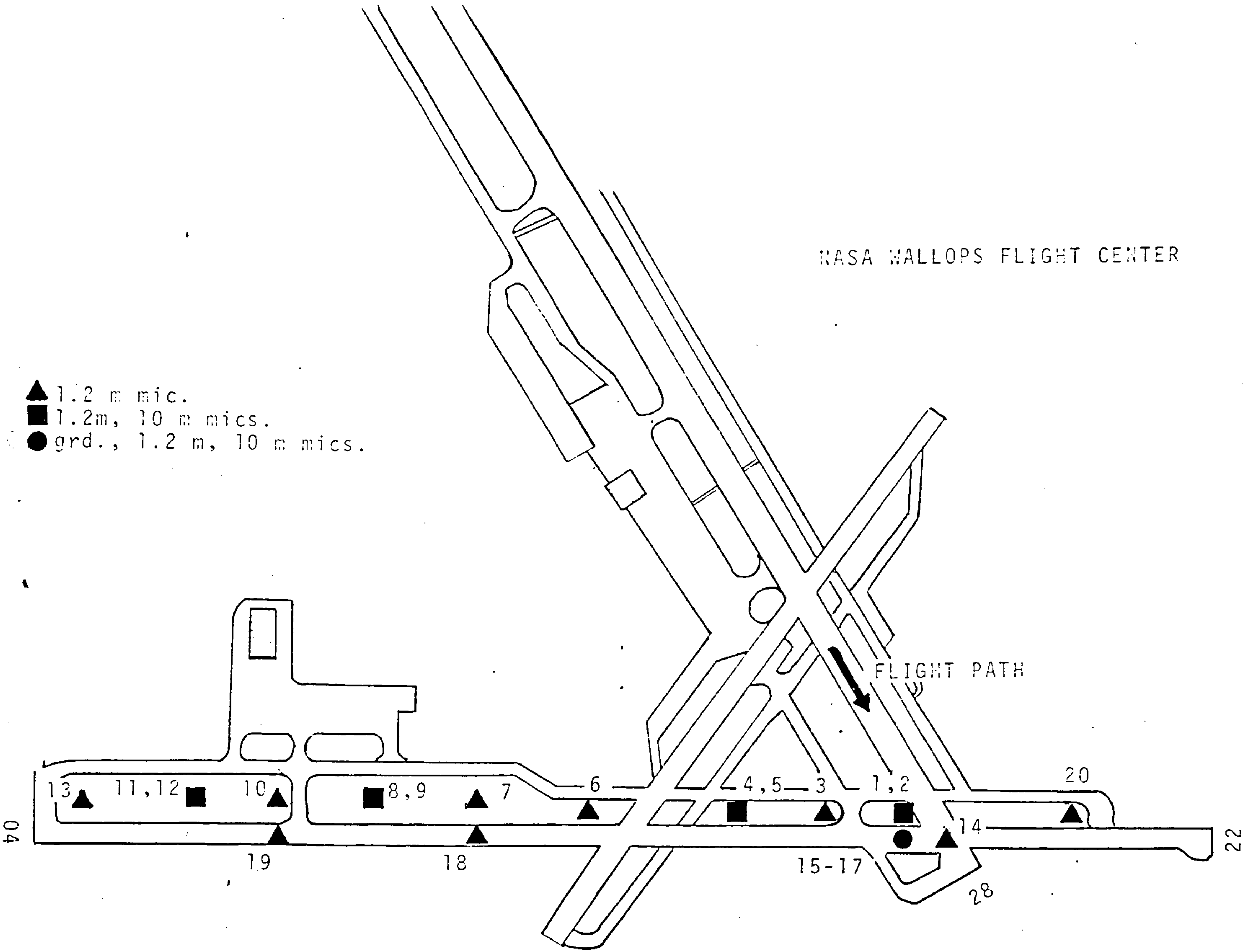

FIGURE 2. MICROPHONE LAYOUT

FIGURE 3. PHOTOGRAPH OF TEST AIRPLANE.

FIGURE 4. PHOTOGRAPH OF TEST AIRPLANE IN FLIGHT.

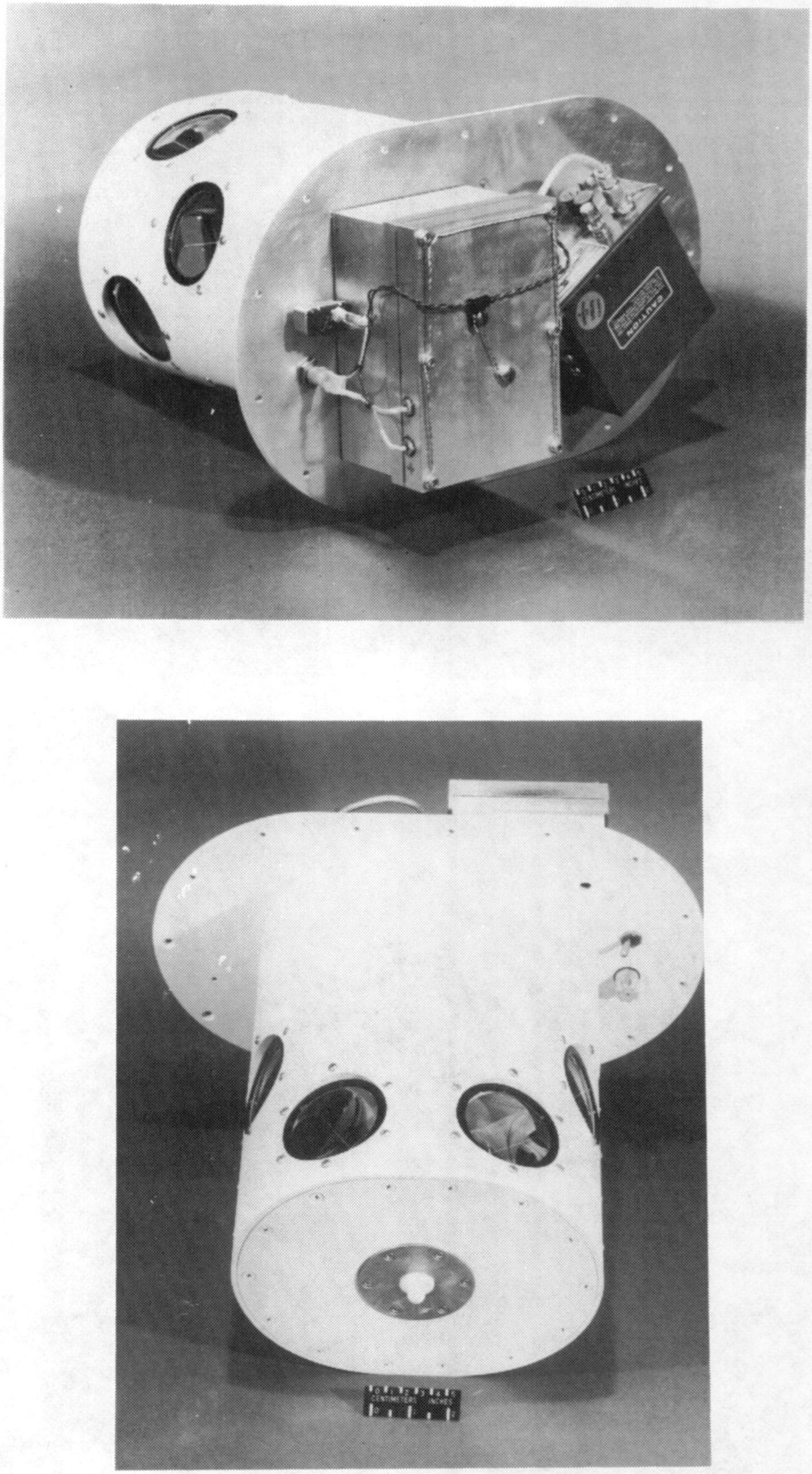

FIGURE 5. LASER REFLECTOR HOUSING.

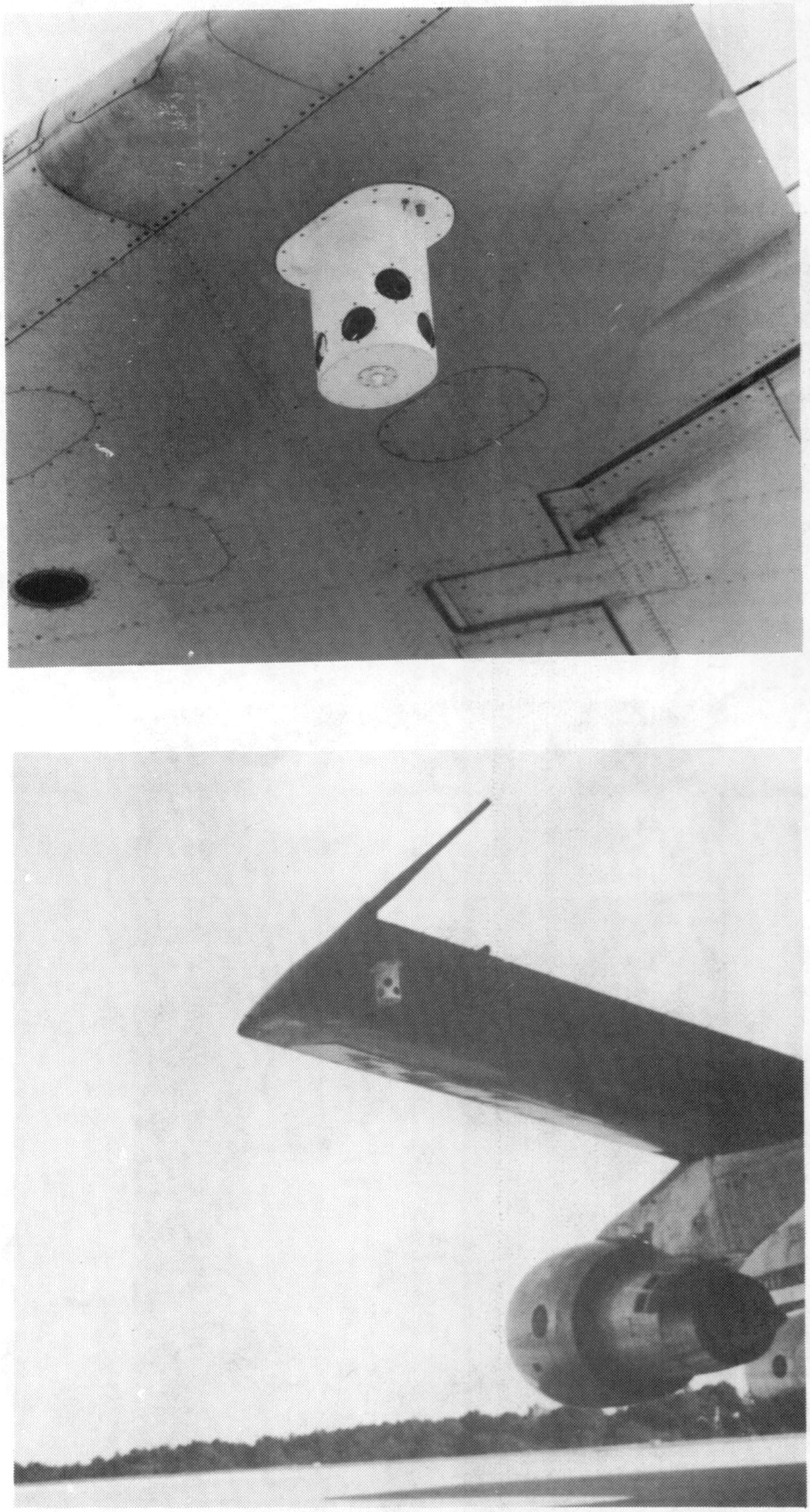

FIGURE 6. LASER REFLECTOR HOUSING INSTALLATION.

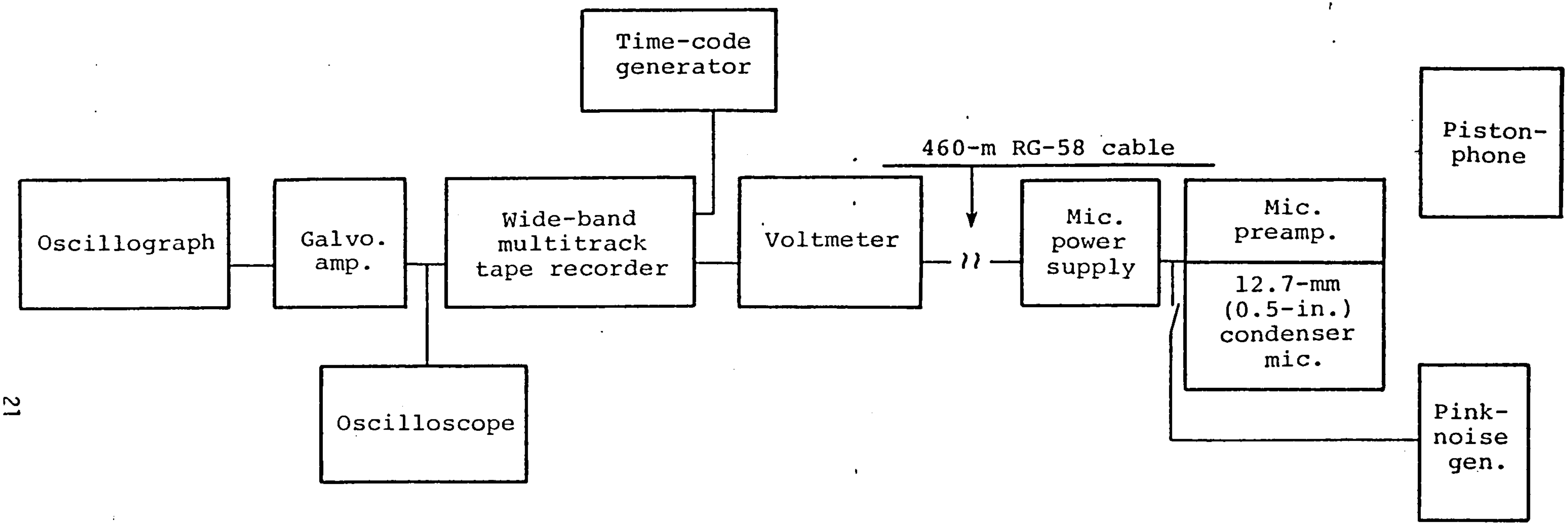

FIGURE 7. BLOCK DIAGRAM OF MICROPHONE SYSTEM.

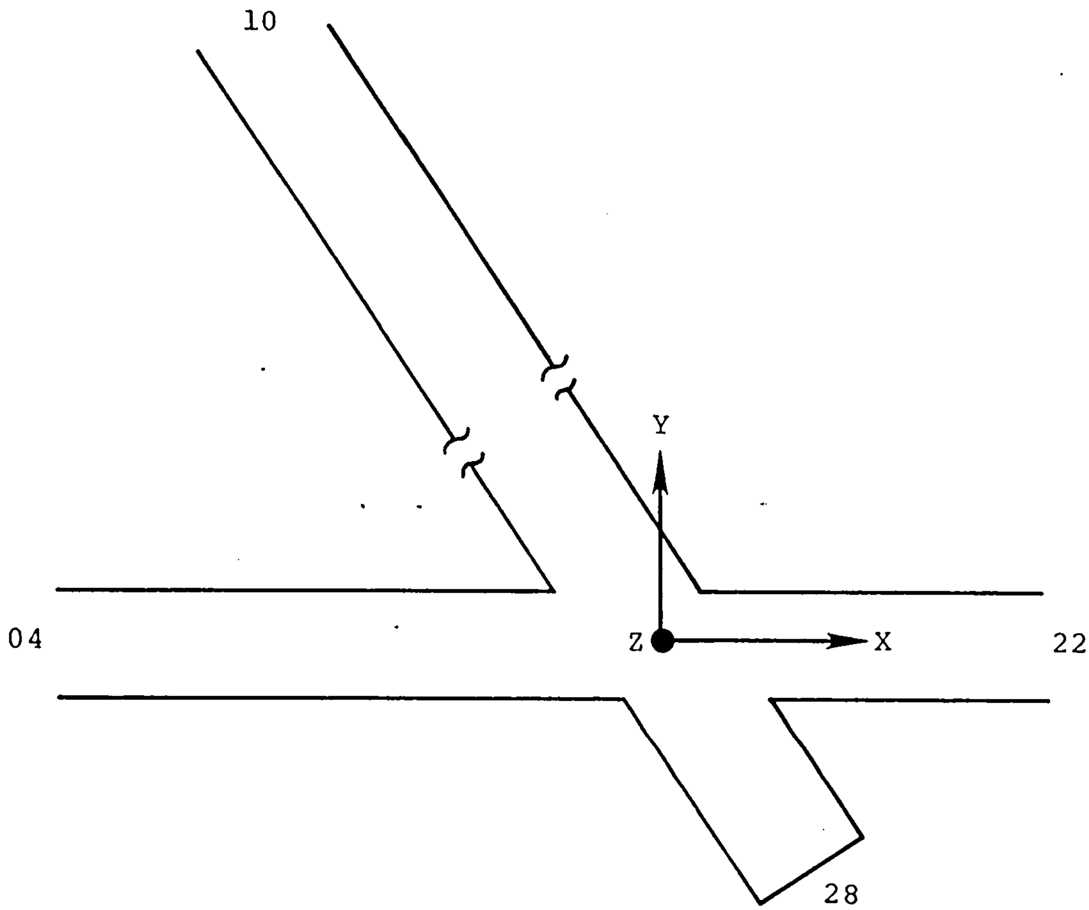

FIGURE 8. DATA REDUCTION COORDINATE SYSTEM.

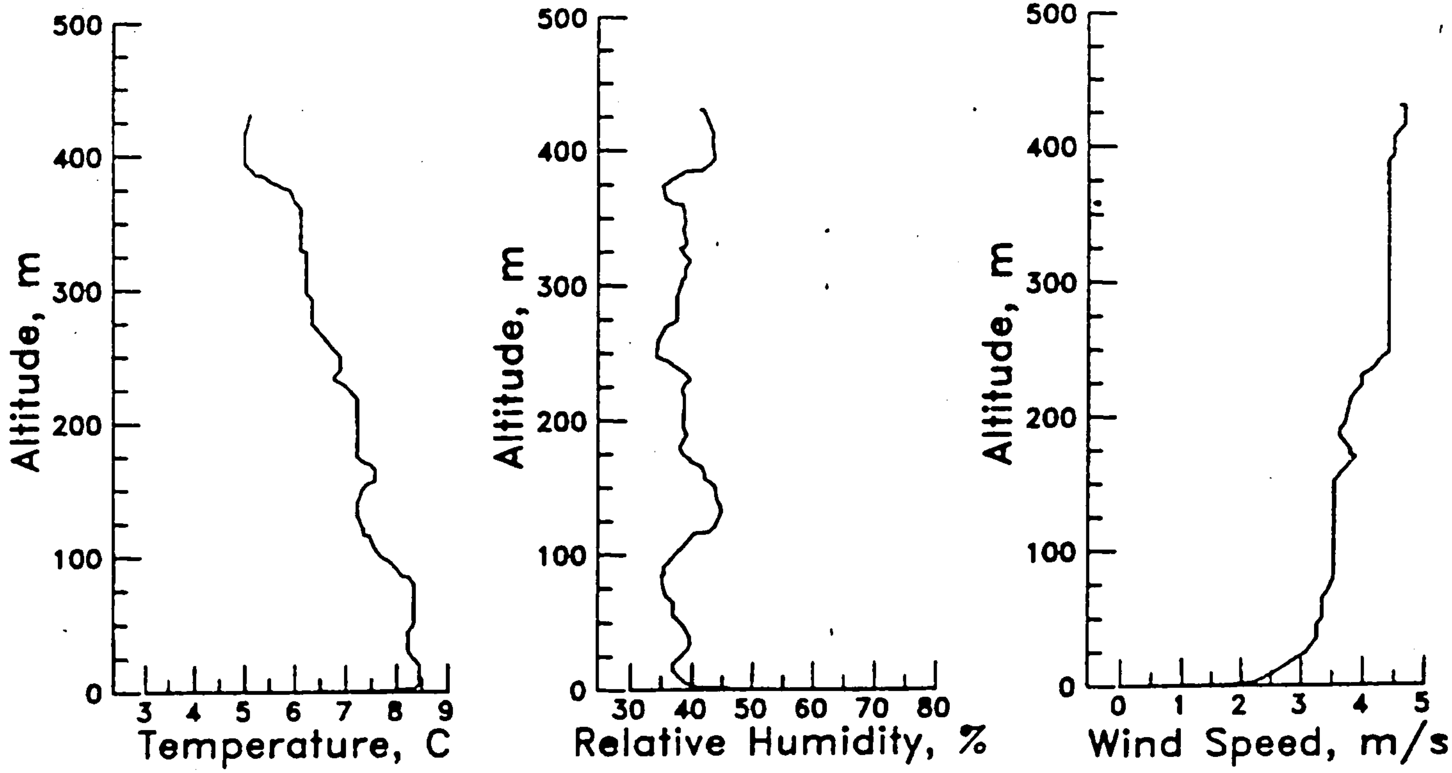

Figure 9. Balloon Weather Profile Data for Run 8

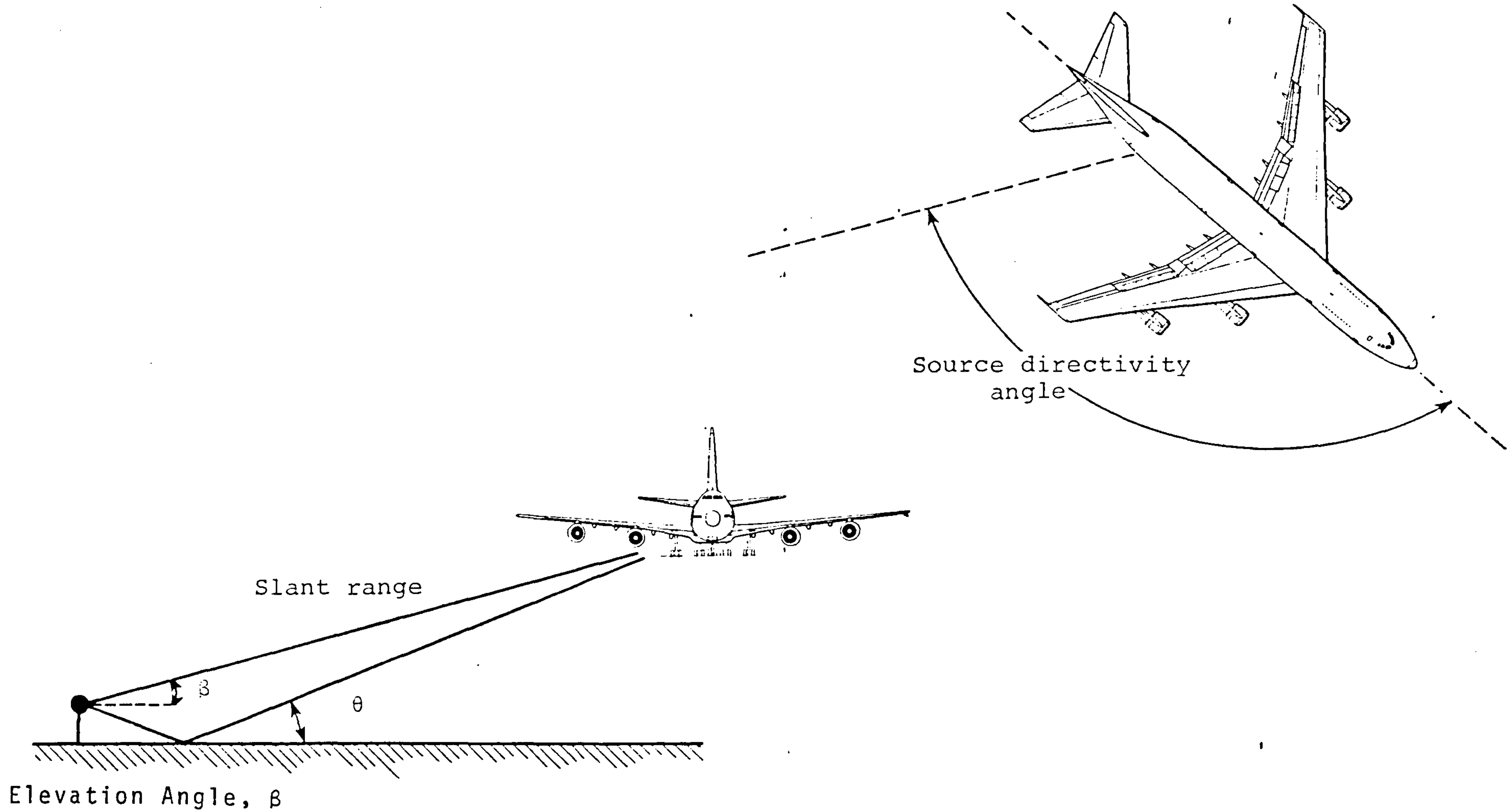

FIGURE 10. SOURCE-MICROPHONE GEOMETRY.

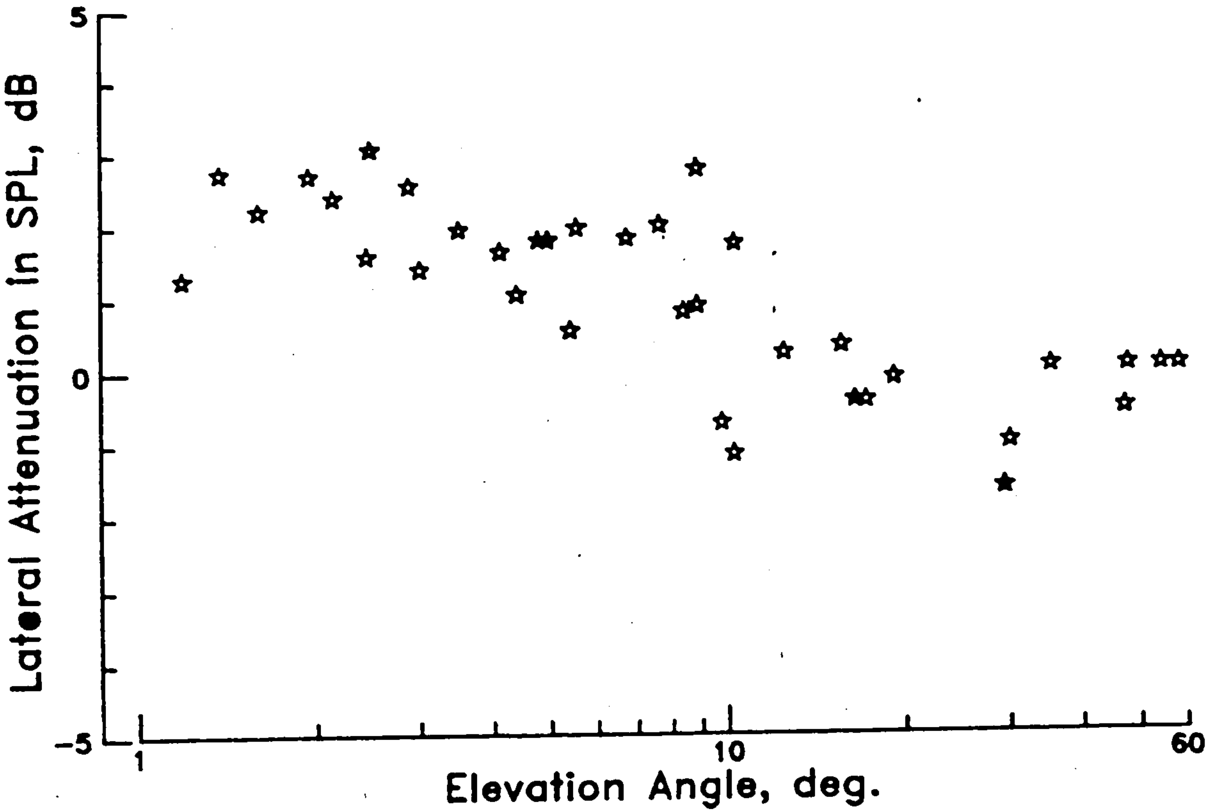

Figure 11. B-747 Lateral Attenuation Results in SPL

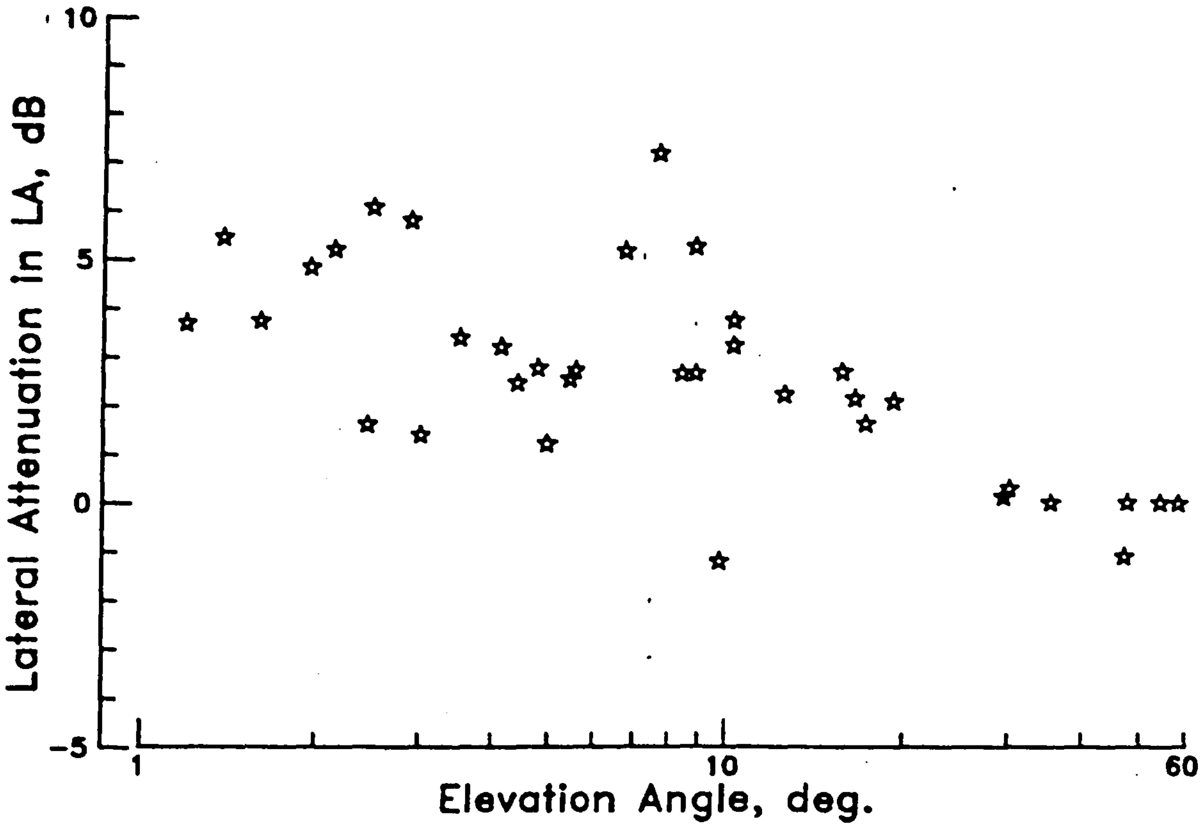

Figure 12. B−747 Lateral Attenuation Results in LA

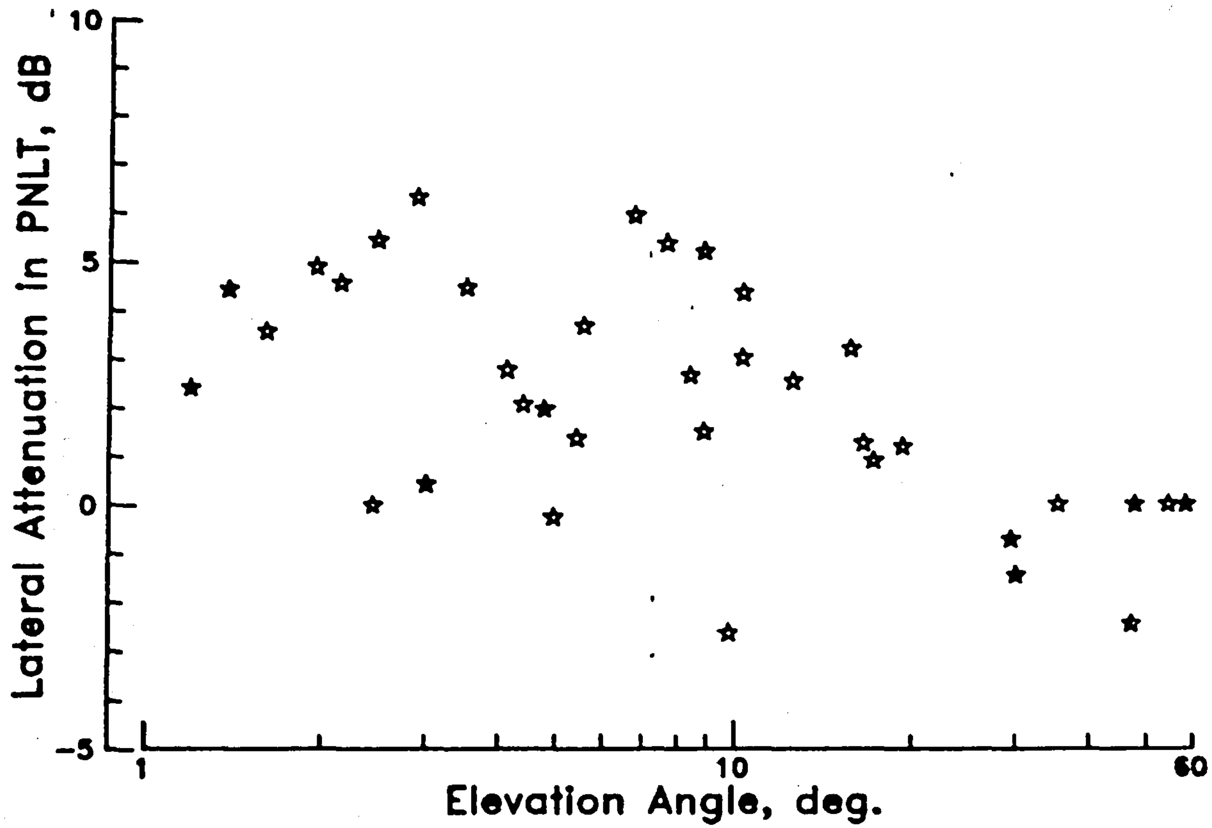

Figure 13. B-747 Lateral Attenuation Results in PNLT

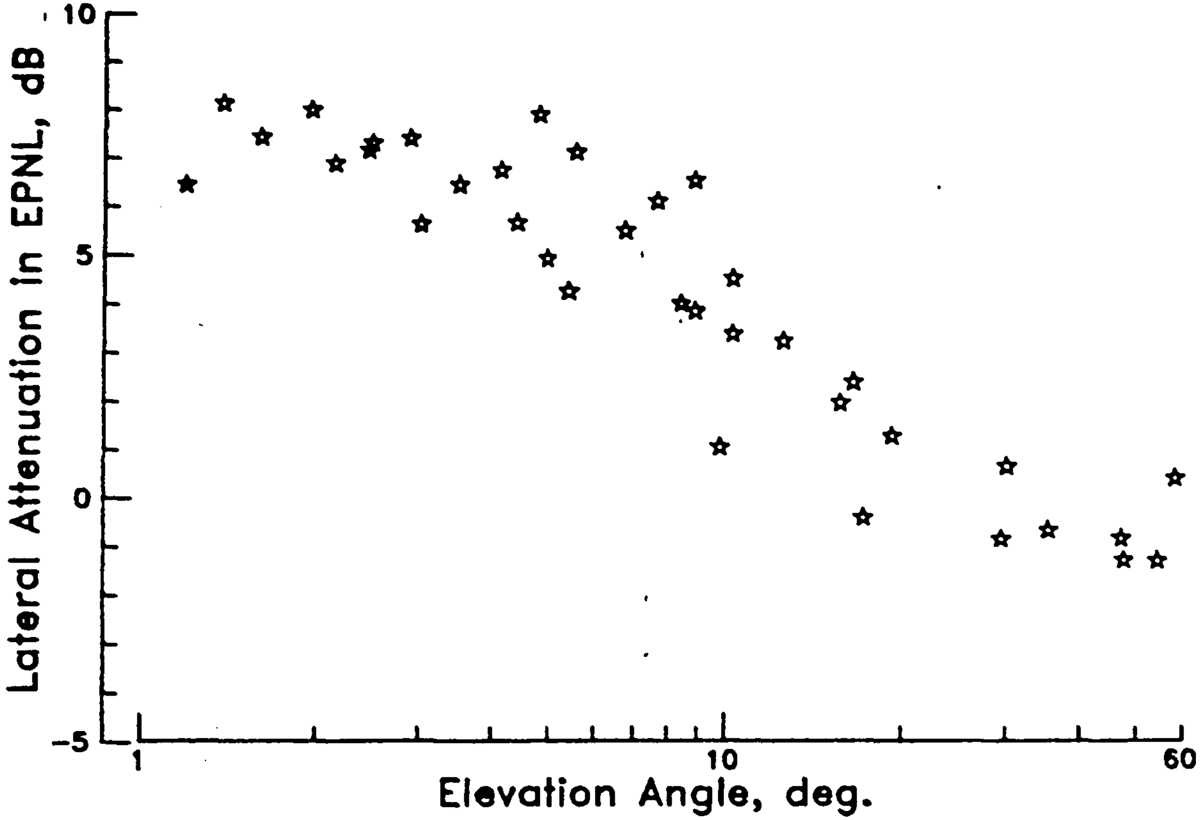

Figure 14. B-747 Lateral Attenuation Results in EPNL

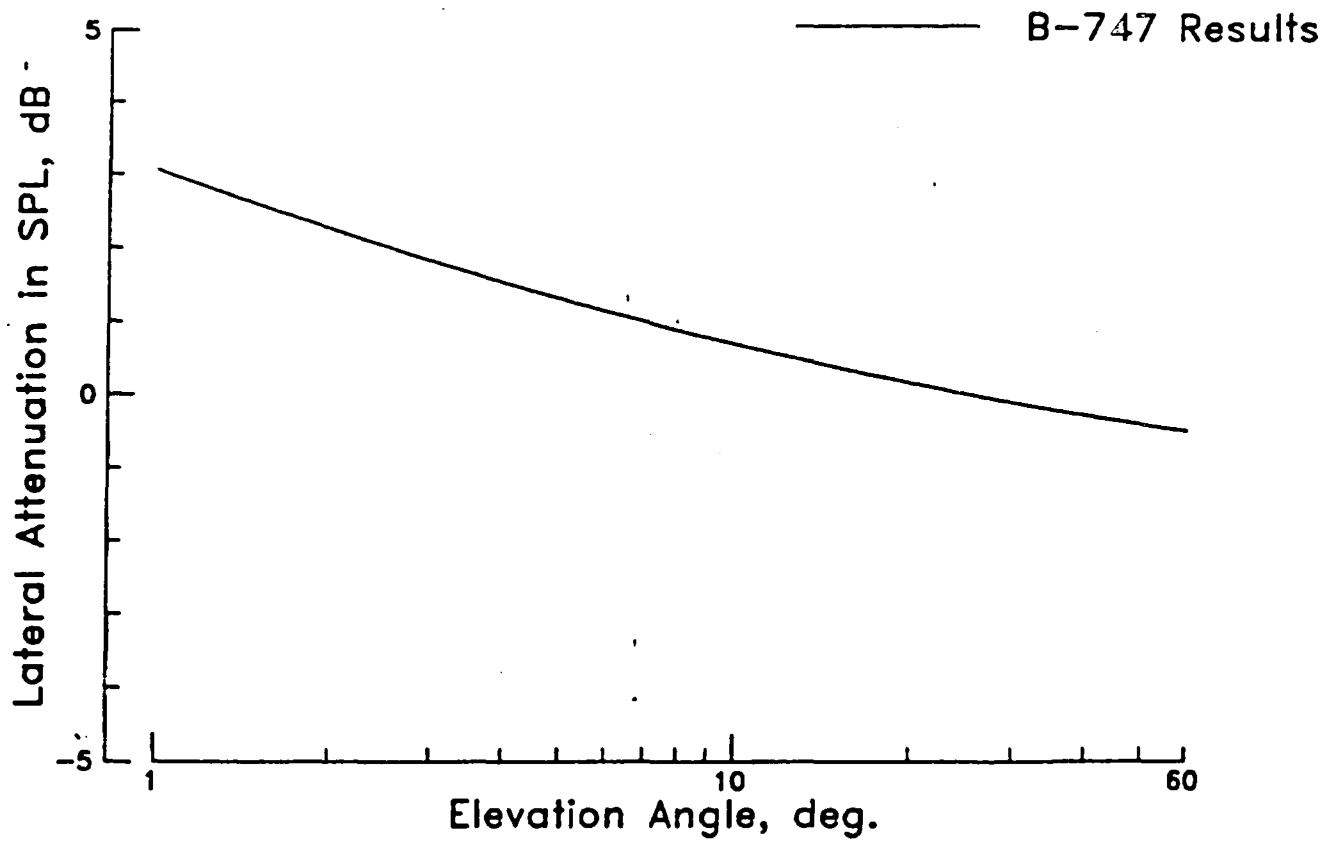

Figure 15. Least-squares Fit of Lateral Attenuation Results in SPL

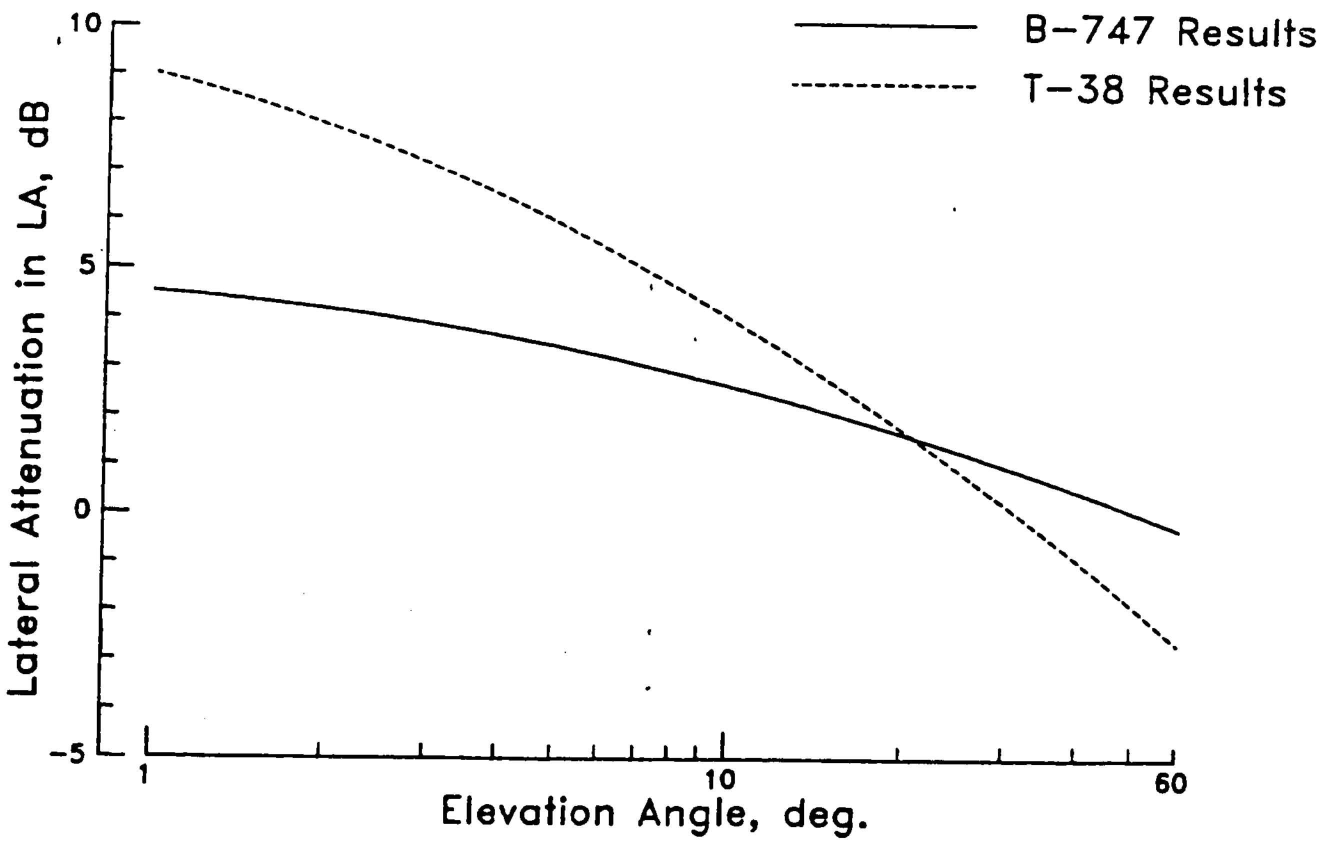

Figure 16. Least−squares Fit of Lateral Attenuation Results in LA

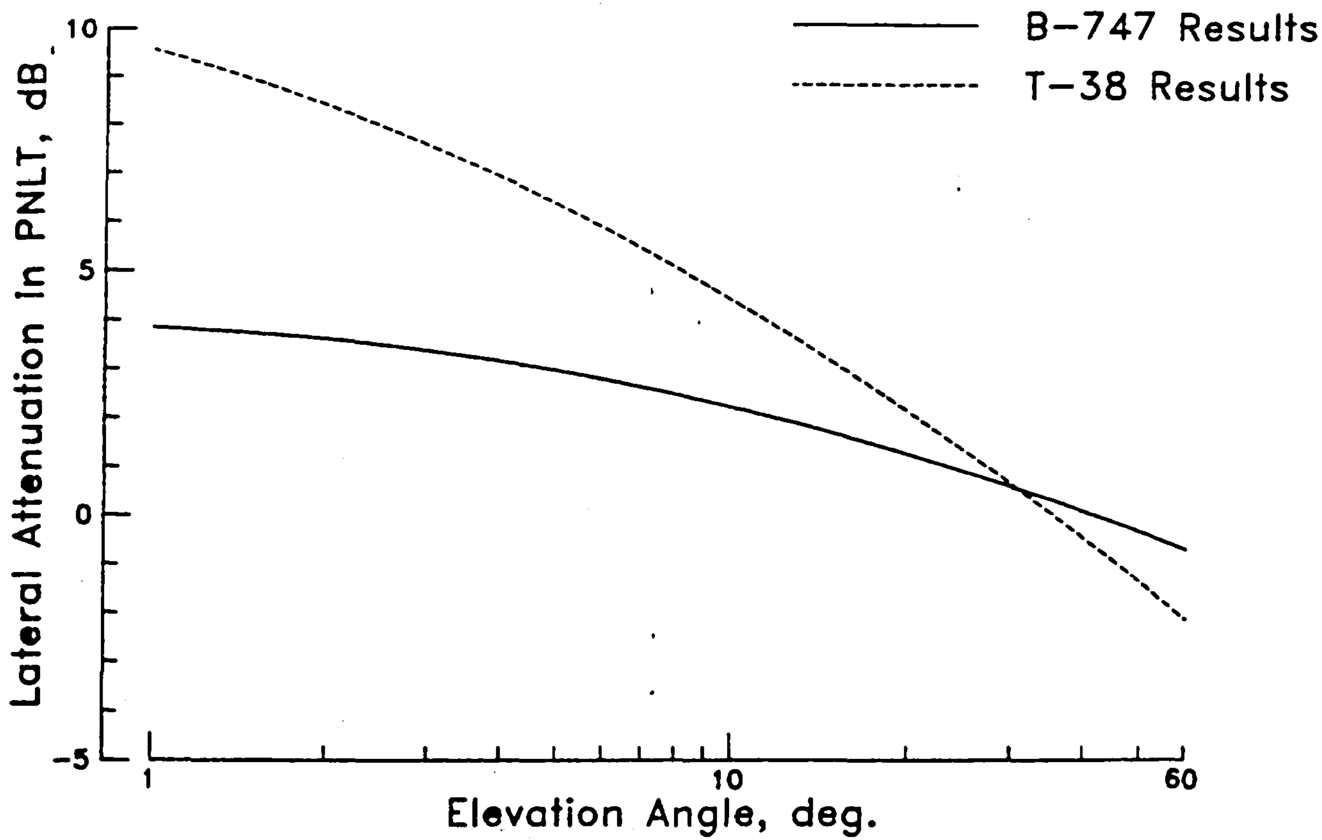

Figure 17. Least-squares Fit of Lateral Attenuation Results in PNLT

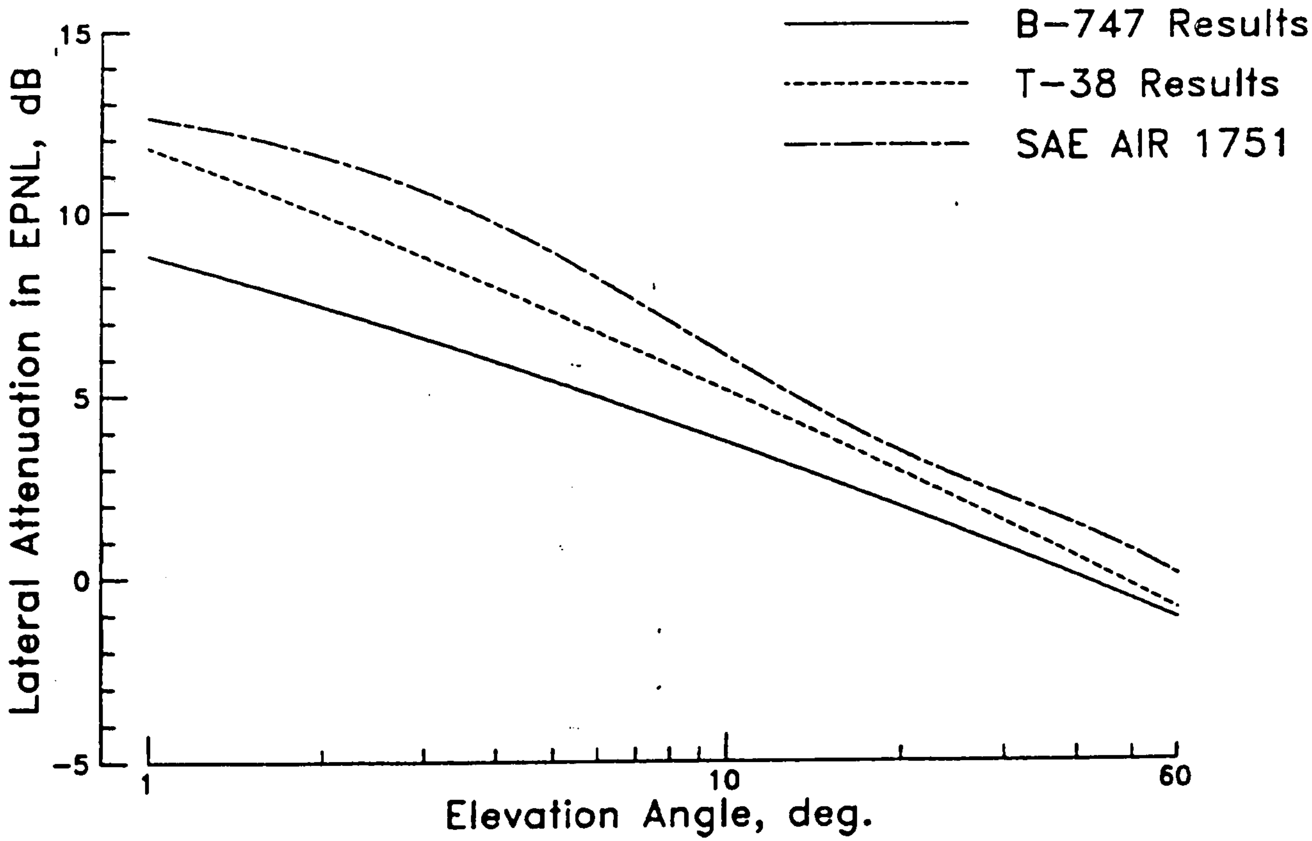

Figure 18. Least−squares Fit of Lateral Attenuation Results in EPNL

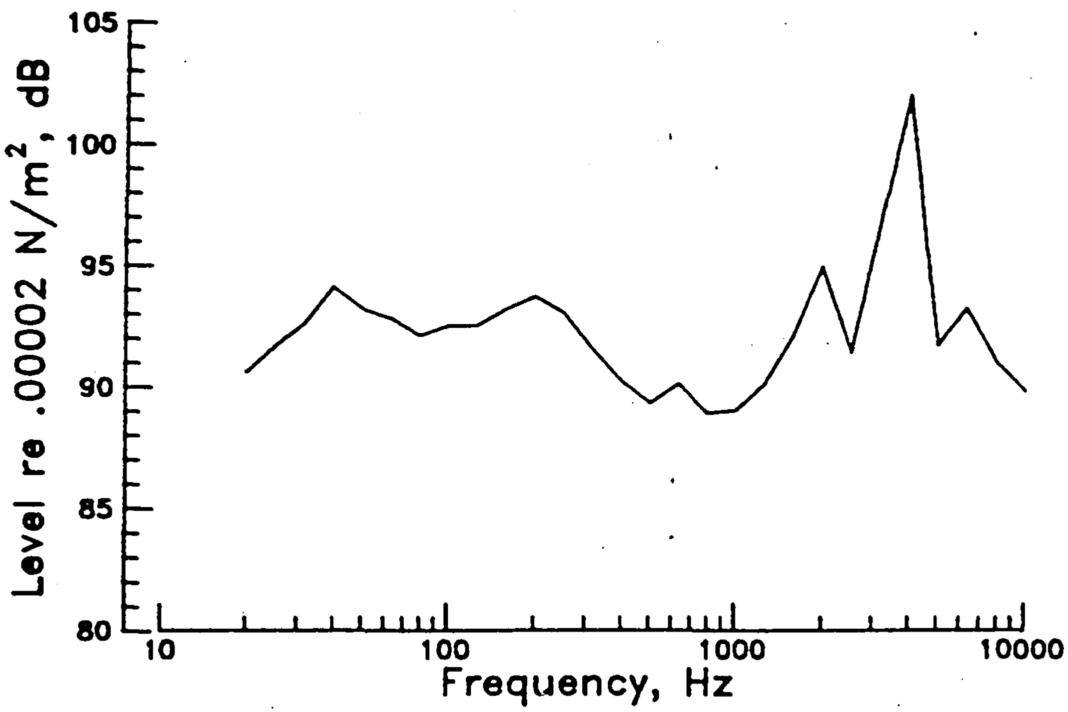

Figure 19. Average B-747 122.5 deg Free-field Spectrum at 50 m

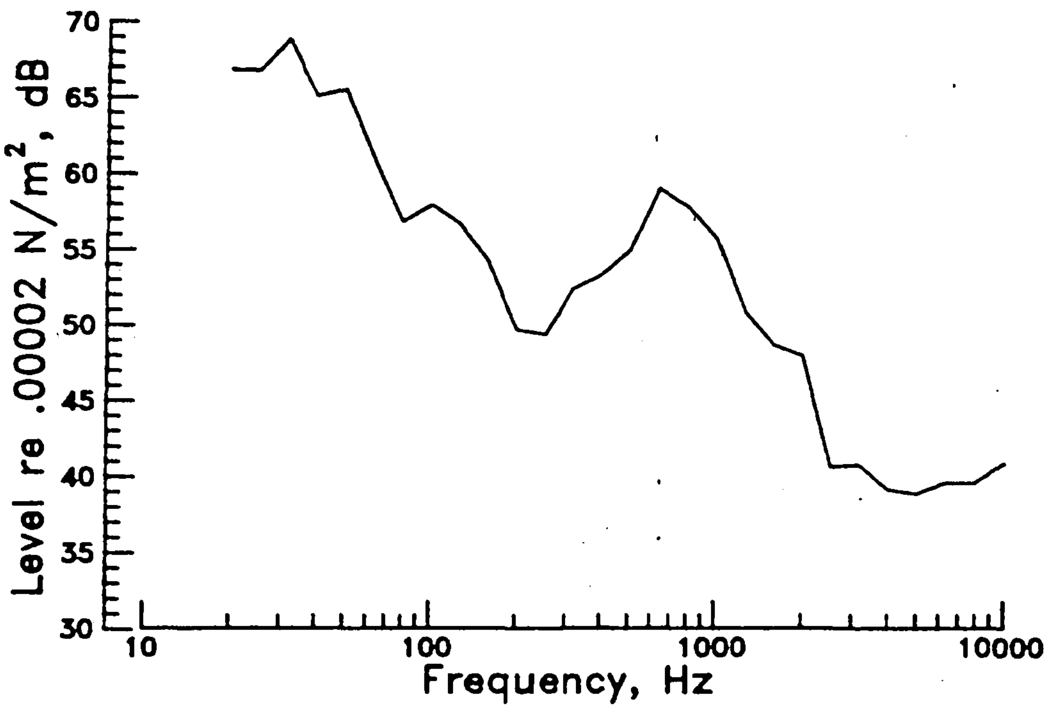

Figure 20. Average B-747 122.5 deg Spectrum for Mic. 10 for 30 m Runs

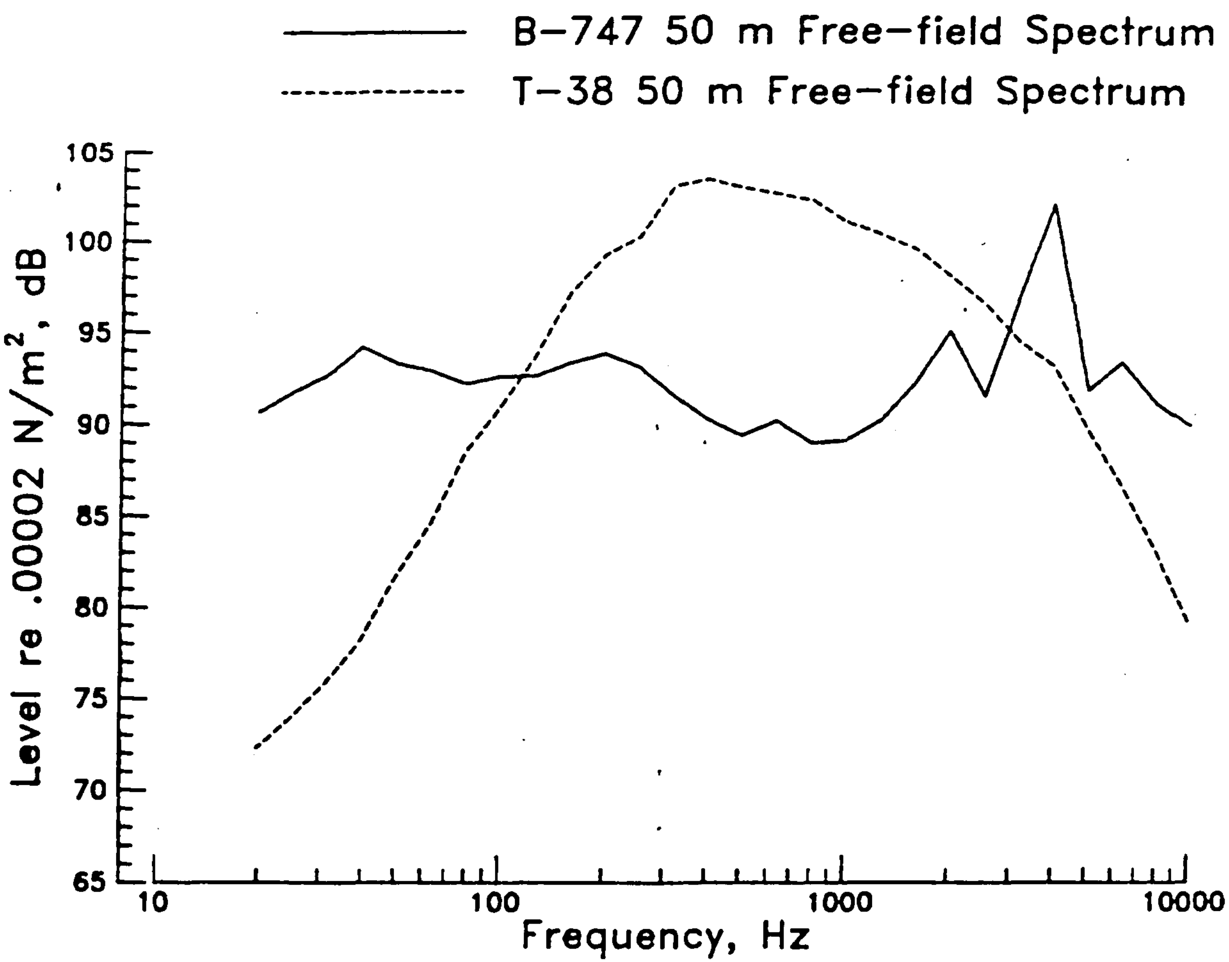

Figure 21. Comparison of B−747 and T−38 Free−field Source Spectra.

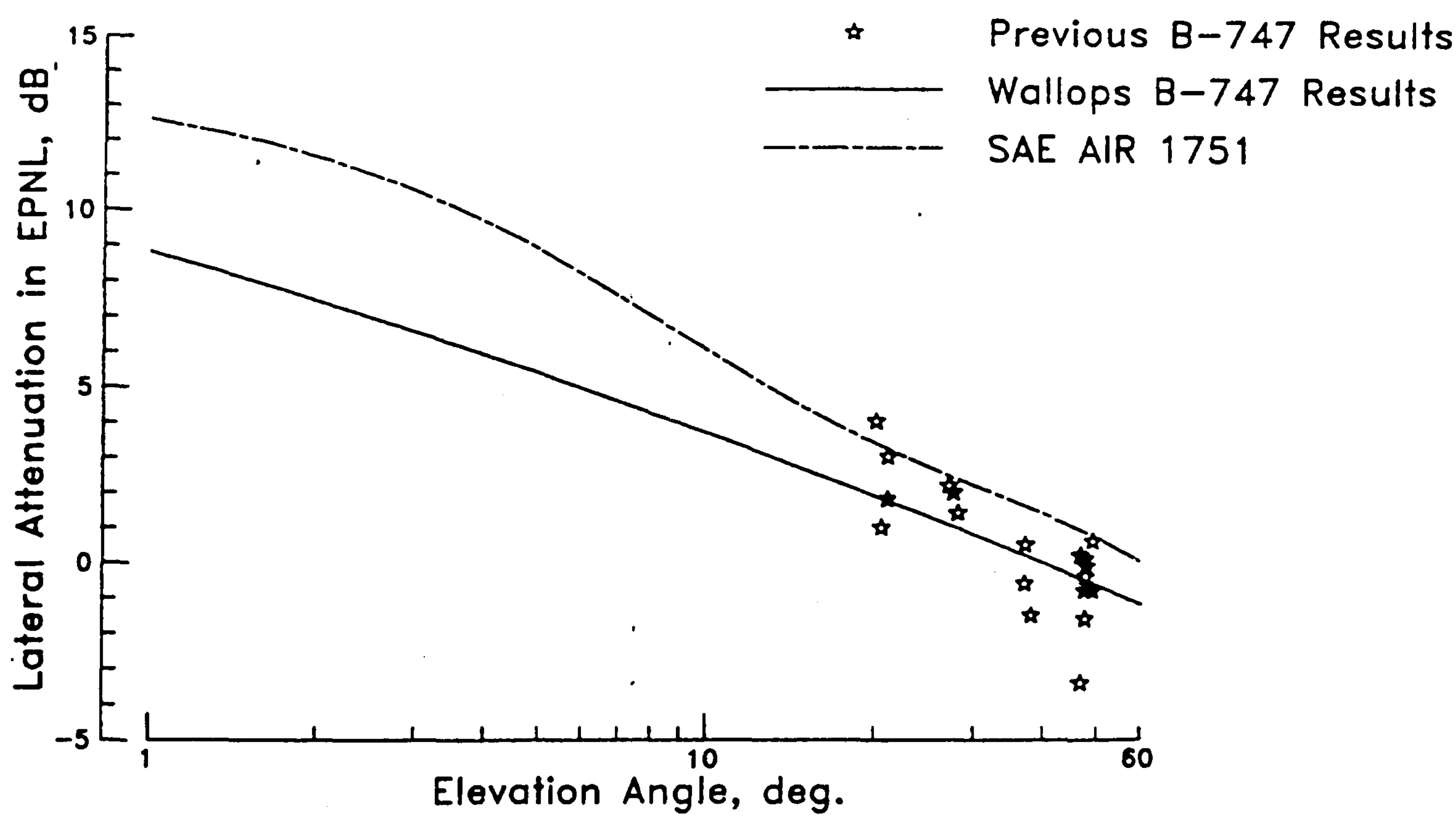

Figure 22. Comparison of B-747 results with SAE AIR 1751 in EPNL

1. Report No.	2. Government Accession No.	3. Recipient's Catalog No.
NASA TM-81968		
4. Title and Subtitle LATERAL ATTENUATION OF HIGH-BY-PASS RATIO ENGINED AIRCRAFT NOISE		5. Report Date April 1981
		6. Performing Organization Code 505-32-03-01
7. Author(s) William L. Willshire, Jr.		8. Performing Organization Report No.
		10. Work Unit No.
9. Performing Organization Name and Address Langley Research Center National Aeronautics and Space Administration Hampton, Virginia 23665		11. Contract or Grant No.
		13. Type of Report and Period Covered Technical Memorandum
12. Sponsoring Agency Name and Address National Aeronautics and Space Administration Washington, D. C. 20546		14. Sponsoring Agency Code

15. Supplementary Notes

16. Abstract

A flight experiment was conducted to investigate the lateral attenuation of high-by-pass ratio engined airplanes. A B-747 was flown at low altitudes over the ends of two microphone arrays. One array covering a lateral distance of 1600 m consisted of 14 microphones positioned over grass. The second array covered a lateral distance of 1200 m and consisted of 6 microphones positioned over a concrete runway. Sixteen runs were flown at altitudes ranging from 30 to 960 m.

The acoustic information recorded in the field has been reduced to one-third-octave band spectral time histories and synchronized with tracking and weather information. Lateral attenuation as a function of elevation angle has been calculated in overall, A-weighted, tone-corrected perceived noise level, and effective perceived noise level units.

The B-747 results are compared with similar results for a turbojet-powered T-38 airplane and the SAE-recommended lateral attenuation prediction procedure. Less lateral attenuation was measured for the B-747 than for the T-38. The B-747 lateral attenuation values also fell below the SAE curve. The B-747 source spectra have considerable energy in the low and high frequencies. The low frequency content was not strongly affected by ground effects or atmospheric absorption and became dominant in the measured spectra.

17. Key Words (Suggested by Author(s))	18. Distribution Statement
Lateral attenuation B-747 Flight experiment one-third-octave	Unclassified - Unlimited Subject Category 71

19. Security Classif. (of this report)	20. Security Classif. (of this page)	21. No. of Pages	22. Price*
Unclassified	Unclassified	36	A03

* For sale by the National Technical Information Service, Springfield, Virginia 22161